

## **A MOUNTAIN-SCALE MODEL FOR CHARACTERIZING UNSATURATED FLOW AND TRANSPORT IN FRACTURED TUFFS OF YUCCA MOUNTAIN**

Yu-Shu Wu, Guoping Lu, Keni Zhang, and G. S. Bodvarsson

Earth Sciences Division  
Lawrence Berkeley National Laboratory  
Berkeley, CA, 94720, USA  
e-mail: [yswu@lbl.gov](mailto:yswu@lbl.gov)

### **ABSTRACT**

This paper presents a recent large-scale modeling study characterizing fluid flow and tracer transport in the unsaturated zone of Yucca Mountain, Nevada, a proposed repository site for storing high-level radioactive waste. This study has been conducted using a three-dimensional numerical model, which incorporates a wide variety of field data and takes into account the coupled processes of flow and transport in Yucca Mountain's highly heterogeneous, unsaturated fractured porous rock. The modeling approach is based on a dual-continuum formulation. Using different conceptual models of unsaturated flow, various scenarios of current and future climate conditions and their effects on the unsaturated zone are evaluated to aid in the assessment of the proposed repository's system performance. These models are calibrated against field-measured data. Model-predicted flow and transport processes under current and future climates are discussed.

### **INTRODUCTION**

In the past two decades, significant progress has been made in characterizing unsaturated flow and transport processes in fractured rock of the unsaturated zone (UZ) of the highly heterogeneous, fractured tuff at Yucca Mountain, Nevada, a proposed permanent subsurface repository for storing high-level radioactive waste. Since the 1980s, extensive field studies of the site have been performed, and many types of data have been collected from the site to investigate flow and transport processes there. Based on field data, a number of numerical models have been developed for evaluating UZ hydrological conditions. Studies before the 1990s primarily used one- and two-dimensional models for understanding basic flow and transport behavior (Rulon et al. 1986; Tsang and Pruess 1987). In the 1990s, Wittwer and co-workers (1992, 1995) started developing a three-dimensional (3-D) model that incorporated many geological and hydrological complexities. Ahlers et al. (1995a; 1995b) and Wu et al. (1996a; 1997) continued the effort of developing the site-scale UZ model with increased spatial resolution and more physical processes, such as gas and heat flow analyses. Since then, more comprehensive model calibrations and studies,

using the mountain-scale numerical model, were made to study liquid flow and radionuclide transport processes in the Yucca Mountain UZ (e.g., Robinson et al., 1996; 1997; Viswanathan et al., 1998; Wu et al., 1999a; 1999b; 2002).

The modeling studies of this paper represent our advances in development of the mountain-scale UZ Flow Model (Wu et al., 2003), which is in turn built on the analysis and results of the above-referenced work as well as many other studies. Different from our previous investigations (Wu et al., 1999a; 1999b; 2002), this work presents more comprehensive 3-D model calibrations using field-measured geochemical isotopic, geothermal, and pneumatic data, in addition to moisture and perched-water data. Moreover, the present model uses a much more refined model grid to characterize the UZ system. Specifically, the current repository design, updated field data, and rock properties are incorporated into this model.

The primary objective of this paper is to summarize the current mountain-scale flow and transport model, i.e., how the model is calibrated. The present work is focused on analyzing flow behavior and patterns in the Yucca Mountain UZ. As application examples, we will apply the model to simulating the ambient hydrological conditions for use in predicting system response to future climate conditions. The emphasis is on how to quantify the moisture flow through the UZ, under present-day and estimated future climate scenarios, and to estimate groundwater travel times from the potential repository to the water table.

### **MODEL DESCRIPTION**

#### **Geological Setting and Model Grid**

The aerial domain of the UZ Model encompasses approximately 40 km<sup>2</sup> of the Yucca Mountain area (Figure 1). The UZ is between 500 and 700 m thick and overlies a relatively flat water table. Yucca Mountain is a structurally complex geological system of Tertiary volcanic rock. Subsurface hydrological processes in the UZ occur in a heterogeneous environment of layered, anisotropic, fractured volcanic tuffs (Scott and Bonk, 1984). The primary geological formations found at Yucca Mountain (from the land

surface down) consist of the Tiva Canyon, Yucca Mountain, Pah Canyon, and the Topopah Spring tuffs of the Paintbrush Group. Underlying these units are the Calico Hills Formation and the Prow Pass, Bullfrog, and Tram Tuffs of the Crater Flat Group (Buesch et al., 1995). These geological formations have been reorganized into hydrogeologic units based primarily on the degree of welding (Montazer and Wilson 1984): the Tiva Canyon welded (TCw) hydrogeologic unit; the Paintbrush nonwelded unit (PTn), consisting primarily of the Yucca Mountain and Pah Canyon members and their bedded tuffs; the Topopah Spring welded (TSw) unit; the Calico Hills nonwelded (CHn); and the Crater Flat undifferentiated (CFu) units.

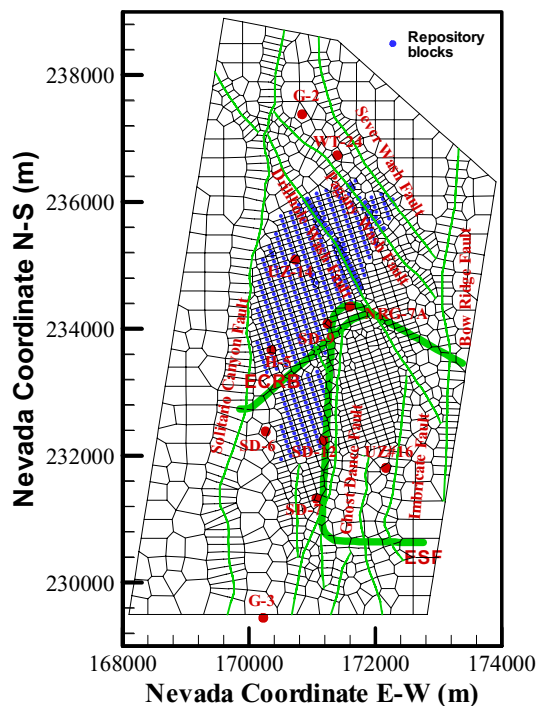


Figure 1. Plan View of the 3-D UZ Model Grid, Showing the Model Domain, Faults Incorporated, Proposed Repository Layout, and Several Borehole Locations

The 3-D mountain-scale UZ model domain, as well as the numerical grid for this study, is shown in plan view in Figure 1. As shown, the UZ model grid is primarily designed for the purpose of model calibrations and investigations of UZ flow behavior. This 3-D model grid uses a refined mesh in the vicinity of the proposed repository, located near the center of the model domain, covering the region from Solitario Canyon to Ghost Dance faults from west to east and north to beyond Pagany Wash fault. Also shown in Figure 1 are the locations of several boreholes used in model calibrations and analyses. The model domain is selected to focus on the study area of the proposed repository and to investigate the effects of different

infiltration scenarios and major faults on moisture flow around and below the proposed repository. In the model grid, faults are represented by vertical or inclined 30 m width zones.

The model grid, as shown in Figure 1, has 2,042 mesh columns (or gridblocks per layer) of both fracture and matrix continua, and averages 59 computational grid layers in the vertical direction, resulting in 250,000 gridblocks and 1,000,000 connections in a dual-permeability grid. This model has a more refined grid numerical resolution than previous mountain-scale models.

### Modeling Approach

Model calibration and simulation results were carried out using TOUGH2 and T2R3D codes (Pruess, 1991; Wu et al., 1996). The single active liquid-phase flow module (EOS9) of the TOUGH2 code was used to calibrate the UZ Flow Model. Tracer transport and chloride studies were performed using the decoupled module of T2R3D, with flow fields generated by the EOS9 module.

Fracture-matrix interactions are handled using a dual-permeability concept to evaluate fluid flow and transport in unsaturated fractured tuffs. When applied, the traditional dual-permeability concept is first modified using an active fracture model (Liu et al., 1998) to represent fingering effects of flow through fractures and to limit flow into the matrix system. Secondly, the dual-permeability grid is modified by adding additional global fracture-matrix connections at the TCw-PTn and PTn-TSw interfaces and at boundaries of vitric units. This provides physical relations for fracture-matrix flow transitions. Note that vitric units in CHn are handled as single-porosity matrix only.

### Boundary Conditions

For the UZ Model, the ground surface of the mountain (or the tuff-alluvium contact in areas of significant alluvial cover) is taken as the top model boundary; the water table is treated as the bottom model boundary. Both the top and bottom boundaries of the model are treated as Dirichlet-type conditions with a specified constant (but spatially distributed) pressure and constant liquid saturation values along these surfaces. For flow simulations using the EOS9 module, only saturation values are specified along the top and bottom model boundaries. Surface infiltration is applied using a source term in the fracture gridblocks within the second grid layer from the top. This is because the first layer is assigned as a Dirichlet-type boundary with constant pressure, saturation, or temperature to represent average atmospheric conditions at the mountain.

All lateral boundaries, as shown in Figure 1, are treated as no-flow (closed) boundaries, which allow for flow along the vertical plan only. Net infiltration from precipitation at land surface is the major control on overall hydrological and thermal-hydrological conditions within the Yucca Mountain UZ. To cover the various possible scenarios and uncertainties of future climates at Yucca Mountain, we have incorporated a total of nine net infiltration maps into the model, provided by US Geological Survey (USGS) scientists (Hevesi and Flint, 2000; Forrester, 2000). These infiltration maps include present-day (modern), monsoon, and glacial transition—three climatic scenarios, each of which consists of lower-bound, mean, and upper-bound rates. The nine infiltration rates are summarized in Table 1 for average values over the model domain.

Table 1. Infiltration Rates (mm/year) Averaged over the Model Domain and Simulation Scenarios

| Scenario           | Lower-Bound Infiltration | Mean Infiltration | Upper-Bound Infiltration |
|--------------------|--------------------------|-------------------|--------------------------|
| Present-Day/Modern | 1.25 (preq_1A)*          | 4.43 (preq_mA)    | 10.74 (preq_uA)          |
| Monsoon            | 4.43 (monq_1A)           | 11.83 (monq_mA)   | 19.23 (monq_uA)          |
| Glacial Transition | 2.35 (glaq_1A)           | 17.02 (glaq_mA)   | 31.69 (glaq_uA)          |

\* Here, code names such as preq\_1A are denoted for simulation case or scenario, with l for lower, m for mean, u for upper bounds, respectively; A represents the base case model.

As shown in Table 1, the average rate for the present-day, mean infiltration with the calibration grid is 4.43 mm/yr distributed over the model domain, which is considered as a base-case infiltration scenario. The use of the lower- and upper-bound infiltration values is intended to cover the uncertainties (associated with the infiltration models) of possible higher or lower rates. The two future climatic scenarios, the monsoon and glacial transition periods, are used to account for possible higher precipitation and infiltration conditions in the future at Yucca Mountain. Note that the glacial transition period has higher infiltration rates except for the lower-bound case. A plan view of the spatial distribution of the present-day mean infiltration maps, as interpolated onto the model grid, is shown in Figure 2. The figure shows patterns of flux distributions with higher infiltration rates in the northern part of the model domain and along the mountain ridge east of the Solitario Canyon Fault from south to north.

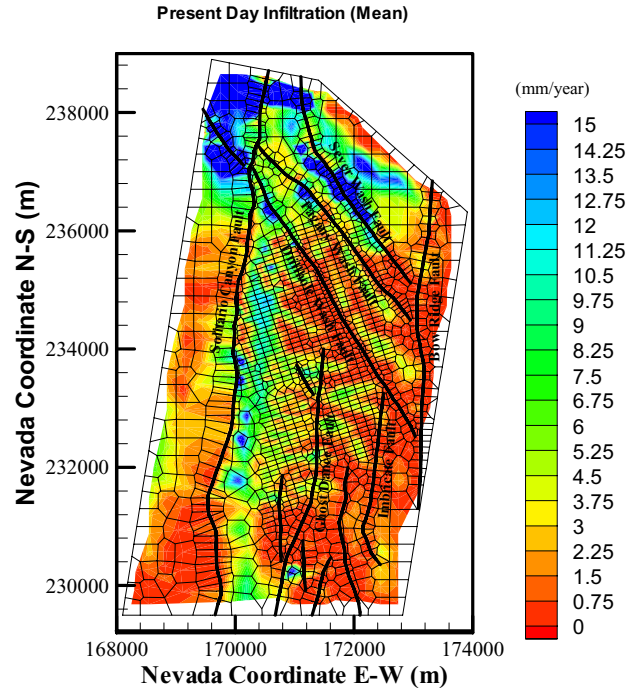


Figure 2. Plan View of Net Infiltration Distributed over the 3-D UZ Flow Model Grid for the Base-Case, or Present-Day, Mean Infiltration Scenario.

### Model Parameters

Input parameters for the rock and fluid properties of each model layer as well as fault-fracture properties are taken from those parameters estimated using a 1-D inversion modeling approach (Liu, 2002). Then the 1-D model estimated properties are calibrated and modified through a series of 3-D model calibrations using field-measured moisture, perched water, pneumatic, temperature, and chloride data. Adopting a hybrid, dual-permeability approach, we treat all of the geological units, including fault zones, as fracture-matrix systems (except for vitric zones).

### MODEL CALIBRATIONS

Model calibration has been a critical step in developing the mountain-scale UZ Model of Yucca Mountain (Wu et al., 1999a and 2002). It is part of the important iterative process of model development and verification, which derives model-scale related parameters and increases confidence in model predictions. While continuing these model calibration studies using a similar methodology, this modeling effort is focused more on an integrated approach to matching all the available hydraulic, geochemical, pneumatic, and geothermal data with a 3-D model. In particular, we only present examples of using moisture and perched water, and chloride data for calibration. The model calibration efforts are conducted to match various types of observation data, thus revealing UZ flow behavior and percolation patterns.

**Comparison with Moisture and Perched Water Data**

Measured matrix liquid saturation, water-potential data, and perched-water elevations from all sampling boreholes have been compared to 3-D model results. This has resulted in model parameter adjustments in several model layers and zones. Simulated and observed matrix liquid saturations and water potentials along the vertical column for borehole SD-12 are compared in Figures 3 and 4, respectively, for the three mean infiltration rates. In general, as shown in Figures 3 and 4, the modeled results from all simulations after calibration are in reasonable agreement with the measured saturation and water-potential profiles, as well as perched water levels.

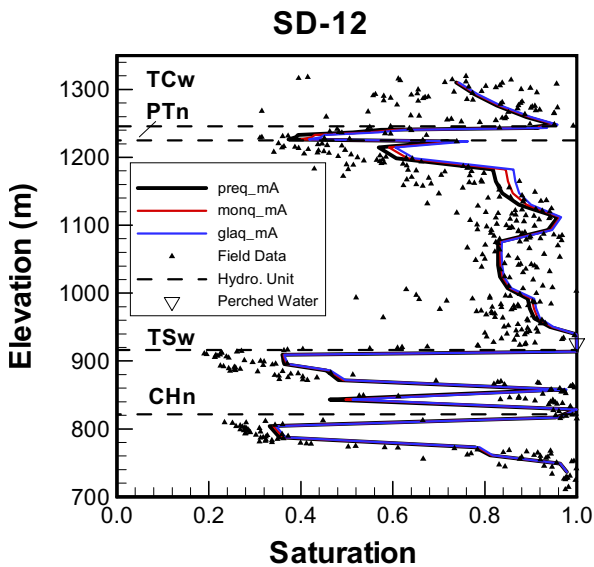


Figure 3. Comparison of Simulated and Observed Matrix Liquid Saturations and Perched-Water Elevations for Borehole SD-12, Using the Results of the Simulations for Three Mean Infiltration Rates.

**Comparison with Chloride Data**

Estimating percolation flux is one of the main objectives of the UZ modeling studies. Water percolation and history data can be analyzed by chemically based natural tracers. Chloride is a nearly ideal natural tracer for the study of water movement in the liquid phase, because it is hydrologically very mobile and chemically inert. Therefore, we use chloride data to calculate infiltration rates along the ESF (Fabryka-Martin et al., 1998; Liu et al., 2003) and specifically to examine possible lateral flow in the PTn unit. The matrix permeability of the PTn is generally several orders of magnitude greater than the overlying TCw, but the degree of fracturing is substantially less. Chloride transport simulations, in conjunction with different infiltration scenarios, are performed to determine possible flow behavior through the PTn by better matching with field samples.

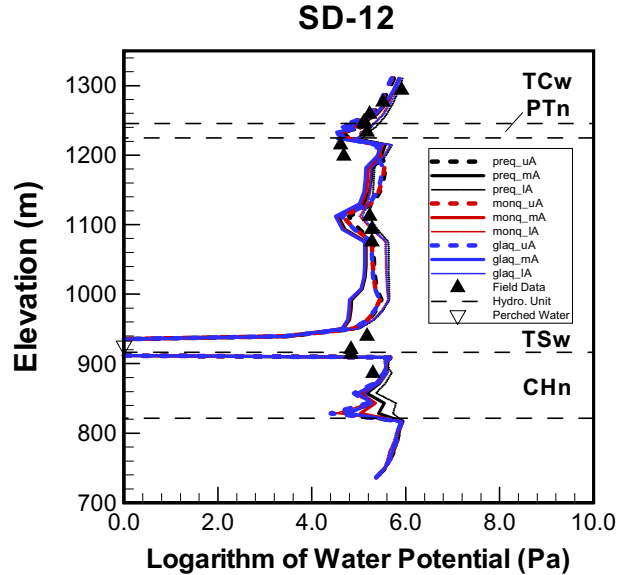


Figure 4. Comparison to Simulated and Observed Matrix Water Potentials and Perched-Water Elevations for Borehole SD-12, Using the Results of the Simulations with Three Mean Infiltration Rates.

The chloride transport simulations considered four scenarios of infiltration: present-day (mean, upper and lower bounds) and glacial mean infiltration. Each scenario is compared to study the effect of lateral flow diversion in the PTn unit, in corresponding to the flow modeling cases. The base case incorporates property sets of the PTn that would more likely cause large-scale lateral flow and the alternative case less likely in comparison. Results show that the chloride transport model representing present-day mean (base-case) infiltration yields the best overall match with field data. In other words, the property set of the PTn that would favor lateral flow diversion (in the PTn unit) matched more closely with the chloride concentration in the field sample. This indicates that lateral diversion may have happened in the PTn unit at Yucca Mountain. Chloride concentrations at different scenarios are plotted in Figure 5. The simulated chloride concentrations from the base-case flow field (preq\_mA, Table 1) in the ESF closely match measured concentrations. Moreover, the simulated chloride concentrations at the glacial-present transitional recharge (glaq\_pmA) fall within the range of samples. This demonstrates again a better match with field data for the glacial scenario (glaq\_pmA), in which the steady-state glacial-present transitional scenarios (run for 110,000 years) switching to the present day recharge for 11,600 years. The trend of chloride concentrations in samples is preserved in the calculated chloride concentrations.

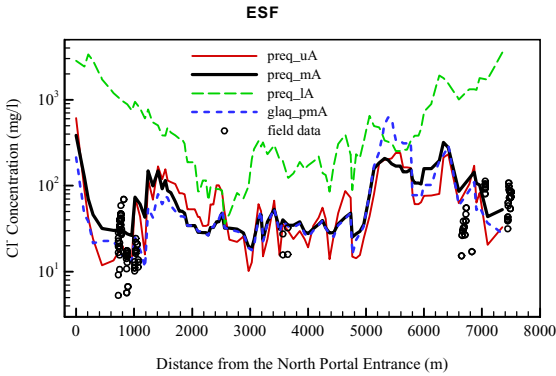


Figure 5. Chloride Concentration (mg/l) Profiles of Present Recharges with Mean, Upper and Lower Bounds  $preq\_mA$ , ( $preq\_uA$ , and  $preq\_lA$ ) and Glacial-Present Transitional Recharge ( $glaq\_pmA$ ) at the ESF.

**FLOW PATTERNS AND ANALYSES**

UZ Flow and Transport Model predictions discussed in this section are presented for insight into flow behavior within the UZ system. These studies are based on the results from 18 3-D, steady-state simulations using the calibrated UZ flow model. Percolation flux through the UZ is considered one of the most critical factors affecting potential repository performance, because of its direct impact on radionuclide mobilization from repository drifts. On the other hand, because percolation fluxes of unsaturated flow cannot be readily measured in the field, they must be estimated using flow models.

**Percolation Flux at Repository**

Percolation fluxes at the repository horizon, as predicted by the current UZ Flow Model, have been analyzed using 18 3-D UZ flow simulation results, with nine infiltration maps (Wu et. al. 2003). Figure 6 shows an example of percolation fluxes simulated at the repository level for the present-day climate. A comparison of the calculated repository percolation fluxes (Figure 6) with the surface infiltration map (Figure 2), described as the top boundary condition, indicates that percolation fluxes at the proposed repository are very different from surface infiltration patterns. This is because a substantial amount of large-scale lateral flow occurs when the percolation flux across the PTn unit.

Percolation fluxes within the repository footprint can be further analyzed using a frequency distribution plot. This plot displays the average percentage of the repository area subject to a particular percolation rate.

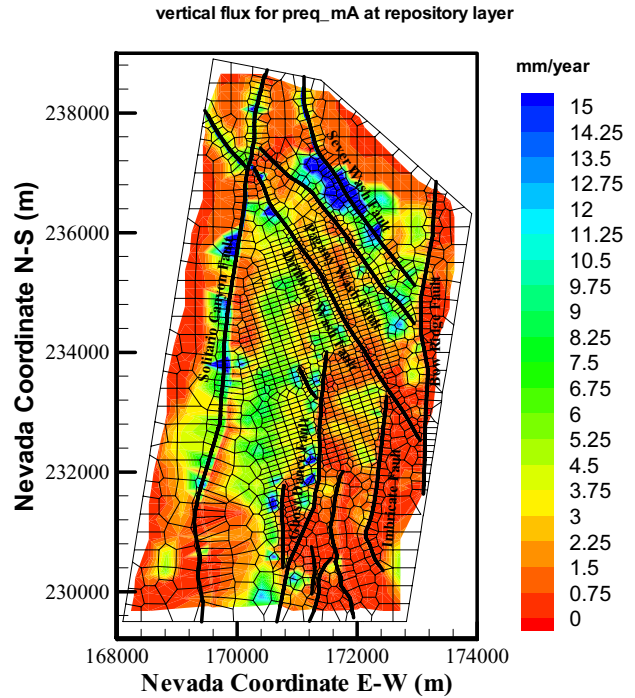


Figure 6. Simulated Percolation Fluxes at the Proposed Repository Horizon under Present-Day, Mean Infiltration Using the Results of Simulation  $preq\_mA$

Note that the normalized flux rates are determined by normalizing an infiltration value with respect to the average infiltration rate for the scenario. For example, 1 for the normalized flux rate corresponds to 4.43, 11.83, and 17.02 mm/yr (Table 1), respectively, for the three mean infiltration scenarios.

The statistical information, as shown in Figure 7, is important to drift-scale modeling studies of flow and transport at drifts and flow-focusing phenomena through the TSw. Figure 7 shows the frequency distribution of normalized percolation flux within the repository horizon for the three mean infiltration rates of the three climates scenarios.

**Groundwater Travel Times**

Tracer-transport-simulation results can also provide insight into flow patterns below the repository using groundwater travel-time analysis. Groundwater travel or trace- transport times are estimated by conservative (nonadsorbing) and reactive (adsorbing) tracer simulations, in which tracers are traced after released from the repository and transported to the water table. Transport simulations are run to 1,000,000 years under 18 3-D steady-state base-case and alternative flow fields. Initially, a tracer with a constant source concentration at the repository is released at the starting time of a simulation.

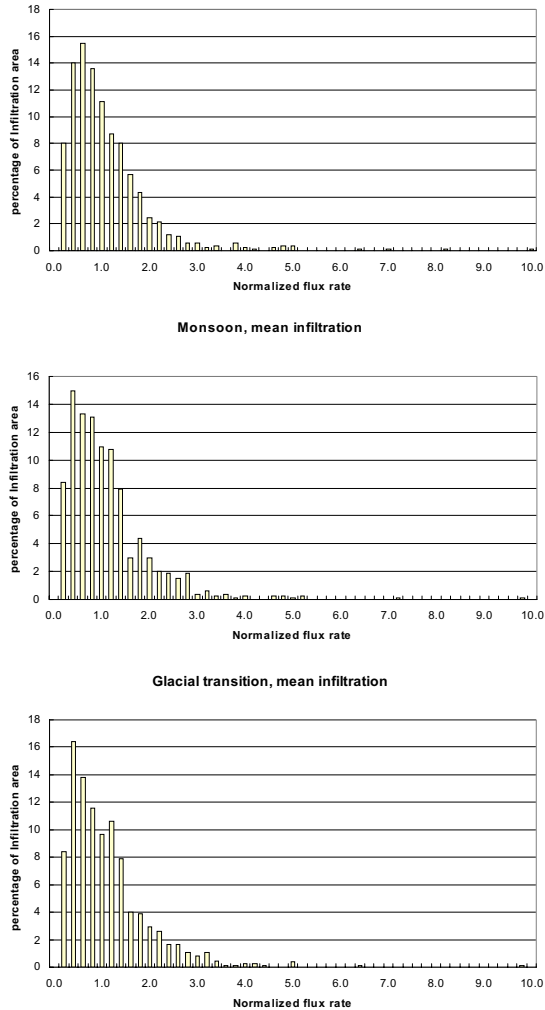


Figure 7. Areal Frequency and Distribution of Simulated Percolation Fluxes within the Proposed Repository Domain, Normalized to the Three Mean Infiltration Rates: (a) Present Day; (b) Monsoon; and (c) Glacial Transition

Groundwater travel times (since release from the proposed repository to the water table) may be analyzed using statistics for groundwater travel or tracer transport times of 50% mass breakthrough at the water table. Figure 8 correlates average infiltration rates and groundwater travel or tracer transport times at 50% mass breakthrough for the 36 simulation scenarios of tracer-fracture release. The statistical data of Figure 8 shows the following:

- Groundwater travel times are inversely proportional to the average surface infiltration (net water recharge) rate. When an average infiltration rate increases from 5 to 35 mm/yr, average groundwater travel (50% breakthrough) times decrease by more than one order of magnitude for both adsorbing and nonadsorbing species.

- Nonadsorbing tracers migrate one to two orders of magnitude faster than an adsorbing tracer when traveling from the proposed repository to the water table under the same infiltration conditions.

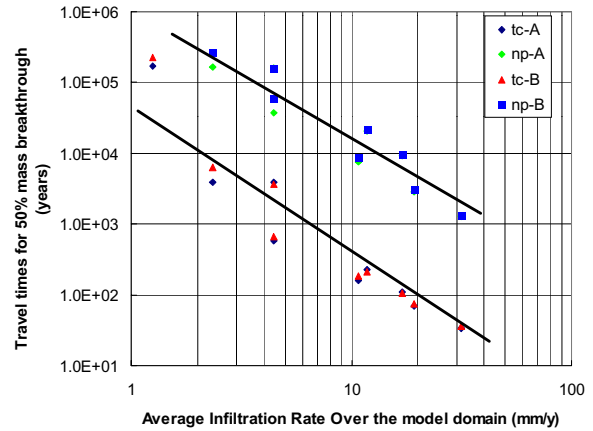


Figure 8. Correlation of Average Infiltration Rates and Groundwater Travel or Tracer Transport Times at 50% Mass Breakthrough for the 36 Tracer-Fracture-Release Simulation Scenarios

## SUMMARY AND CONCLUSIONS

This paper presents an updated 3-D mountain-scale UZ Flow Model, developed for characterizing fluid flow and tracer/radionuclide transport in the UZ of Yucca Mountain. The UZ model has been calibrated using an integrated approach of incorporating a wide range of available data observed and measured from the site, including field-measured saturation, water-potential and perched-water information, temperature profiles, and pneumatic and geochemical data. These model-calibration efforts enable us to conclude that the model can predict such moisture conditions in the Yucca Mountain UZ system as liquid saturation, water potential, and perched water occurrence.

Modeling results calibrated using chloride data indicate possible flow diversion and focusing into faults in the vicinity of the potential repository. Faults act as major flow paths through the CHn in the northern part of the model domain under the current conceptualization. Tracer-transport studies indicate that there exists a wide range of simulated tracer-transport times, associated mainly with different infiltration rates and modeling scenarios. Sensitivity analyses indicate that surface infiltration rates and adsorption effects in the CHn unit are the most important factors for determining tracer-transport times.

## ACKNOWLEDGMENTS

The authors would like to thank Guoxiang Zhang and Dan Hawkes for their review of this paper. In addition, the authors are grateful to Lehua Pan and H. H. Liu for providing input to this work. This work was supported by the Director, Office of Civilian Radioactive Waste Management, U.S. Department of Energy, through Memorandum Purchase Order EA9013MC5X between Bechtel SAIC Company, LLC and the Ernest Orlando Lawrence Berkeley National Laboratory (Berkeley Lab). The support is provided to Berkeley Lab through the U.S. Department of Energy Contract No. DE-AC03-76SF00098

## REFERENCES

Ahlers C.F., Bandurraga, T. M., Bodvarsson, G. S., Chen, G., Finsterle, S. and Wu., Y. S., 1995a. Summary of model calibration and sensitivity studies using the LBNL/USGS Three-Dimensional Unsaturated Zone Site-Scale Model, Yucca Mountain Site Characterization Project Report.

Ahlers C.F., Bandurraga, T. M., Bodvarsson, G. S., Chen, G., Finsterle, S. and Wu., Y. S., 1995b. Performance analysis of the LBNL/USGS three-dimensional unsaturated zone site-scale model, Yucca Mountain Project Milestone 3GLM105M, Lawrence Berkeley National Laboratory, Berkeley, CA.

Buesch, D. C.; Spengler, R. W.; Nelson, P.H.; Vaniman, D.T.; Chipera, S.J.; and Bish, D.L. 1995. Geometry of the Vitric-Zeolitic Transition in Tuffs and the Relation to Fault Zones at Yucca Mountain, Nevada. *International Union of Geodesy and Geophysics, XXI General Assembly, July 2-14, 1995*, A426.

Fabryka-Martin, J.T., A.V. Wolfsberg, J.L. Roach, S.T. Winters, L.E. Wolfsberg, 1998, Using chloride to trace water movement in the unsaturated zone at Yucca Mountain, Proceedings of the 8<sup>th</sup> Annual International High Level Radioactive Waste Management Conference, American Nuclear Society, La Grange Park, IL.

Forrester, R., 2000. Future Climate Analysis. Report ANL-NBS-HS-000032. Denver, Colorado: U. S. Geological Survey.

Hevesi, J. and Flint, L., 2000. Simulation of Net Infiltration for Modern and Potential Future Climate. Report ANL-NBS-GS-000008. Denver, Colorado: U. S. Geological Survey.

Liu, H. H., 2002, *Calibrated Properties Model*. MDL-NBS-HS-000003 REV 01, Las Vegas, Nevada: Bechtel SAIC Company.

Liu, H. H., Doughty, C., and Bodvarsson, G. S., 1998, An active fracture model for unsaturated flow and transport in fractured rocks, *Water Resource Research*, v. 34, pp.2633–2646.

Liu, J., E.L. Sonnenthal, and G.S. Bodvarsson, 2003, Calibration of Yucca Mountain unsaturated zone flow and transport model using porewater chloride data, *Journal of Contam. Hydrol.* (special issue) (in press).

Montazer, P. and Wilson, W. E., 1984. *Conceptual Hydrologic Model of Flow in the Unsaturated Zone, Yucca Mountain, Nevada*. Water-Resources Investigations Report 84-4345. Lakewood, Colorado: U.S. Geological Survey.

Pruess, K., 1991. *TOUGH2-A General-Purpose Numerical Simulator for Multiphase Fluid and Heat Flow*. LBL-29400, Berkeley, California: Lawrence Berkeley Laboratory.

Robinson, B. A., Wolfsberg, A. V., Viswanathan, H. S., Bussod, G., Gable, C. G., and Meijer, A, 1997. *The Site-Scale Unsaturated Zone Transport Model of Yucca Mountain*. Las Alamos National Laboratories. Milestone SP25BMD, Las Alamos, New Mexico: Las Alamos National Laboratories.

Robinson, B. A., Wolfsberg, A. V., Viswanathan, H. S., Gable, C. W., Zyvoloski, G. A., and Turin, H. J. 1996. *Modeling of Flow Radionuclide Migration and Environmental Isotope Distributions at Yucca Mountain*. Las Alamos National Laboratories. Milestone 3672, Las Alamos, New Mexico: Las Alamos National Laboratories.

Rousseau J. P., Kwicklis, E. M. and Gillies, C. eds, 1998. Hydrogeology of the unsaturated zone, North Ramp area of the Exploratory Studies Facility, Yucca Mountain, Nevada, U.S. Geological Survey, Water-Resources Investigations 98-4050.

Rulon, J., Bodvarsson, G. S. and Montazer, P., 1986. *Preliminary Numerical Simulations of Groundwater Flow in the Unsaturated Zone, Yucca Mountain, Nevada*. LBL-20553. Berkeley, California: Lawrence Berkeley Laboratory.

Scott, R. B. and Bonk, J., 1984. *Preliminary Geologic Map of Yucca Mountain, Nye County, Nevada, with Geologic Sections*. Open-File Report 84-494. Denver, Colorado: U.S. Geological Survey.

Tsang, Y. W. and Pruess, K., 1987. A study of thermally induced convection near a high-level nuclear waste repository in partially saturated fracture tuff, *Water Resources Research*, 23(10), pp.1958-1966.

Viswanathan, H. S., Robinson, B. A., Valocchi, A. J., and Triay, I. R. 1998. A Reactive Transport Model of Neptunium Migration from the Potential Repository at Yucca Mountain, *Journal of Hydrology*, 209, pp. 251-280.

Wittwer, C., Chen, G., Bodvarsson, G. S., Chornack, M., Flint, A., Flint, L., Kwicklis, E., and Spengler, R., 1995. *Preliminary Development of the LBL/USGS Three-Dimensional Site-Scale Model of Yucca Mountain, Nevada*. LBL-37356. Berkeley, California: Lawrence Berkeley Laboratory.

Wittwer, C. S.; Bodvarsson, G. S.; Chornack, M. P.; Flint, A. L.; Flint, L. E.; Lewis, B. D.; Spengler, R. W. and Rautman, C. A. 1992. Design of a Three-Dimensional Site-Scale Model for the Unsaturated Zone at Yucca Mountain, Nevada. *High Level Radioactive Waste Management, Proceedings of the Third International Conference, Las Vegas, Nevada, April 12-16, 1992*. 1, pp.263-271.

Wu, Y. S., Lu, G, Zhang, K., Zhang, G., Liu, H. H., Xu, T., and Sonnenthal, E., 2003. UZ Flow Models and Submodels, MDL-NBS-HS-000006 REV 01, Las Vegas, Nevada: Bechtel SAIC Company.

Wu, Y. S. and Pruess K., 2000. Numerical Simulation of Non-Isothermal Multiphase Tracer Transport in Heterogeneous Fractured Porous Media, *Advance in Water Resources*, Vol. 23, pp. 699-723.

Wu, Y.S.; Haukwa, C.; and Bodvarsson, G. S., 1999a. A Site-Scale Model for Fluid and Heat Flow in the Unsaturated Zone of Yucca Mountain, Nevada. *Journal of Contaminant Hydrology*. 38 (1-3), pp.185-217.

Wu, Y. S.; Ritcey, A. C.; and Bodvarsson, G. S., 1999b. A Modeling Study of Perched Water Phenomena in the Unsaturated Zone at Yucca Mountain. *Journal of Contaminant Hydrology*. 38 (1-3), pp.157-184.

Wu, Y-S.; Zhang, W.; Pan, L.; Hinds, J.; and Bodvarsson, G.S. 2000. *Capillary Barriers in Unsaturated Fractured Rocks of Yucca Mountain, Nevada*. LBNL-46876. Berkeley, California: Lawrence Berkeley National Laboratory. TIC: 249912.

Wu, Y.S.; Pan, L., Zhang, W. and Bodvarsson, G.S. 2002. "Characterization of Flow and Transport Processes within the Unsaturated Zone of Yucca Mountain, Nevada ." *Journal of Contaminant Hydrology* 54, 215-247. Amsterdam, The Netherlands: Elsevier Science Publishers.

Wu, Y. S., Ritcey, A. C., Haukwa, C. and Bodvarsson, G. S., 1997. Integrated 3-D Site-Scale Flow Model, Chapter 19 of "The Site-Scale Unsaturated Zone Model of Yucca Mountain, Nevada, for the Viability Assessment" Edited by G.

S. Bodvarsson, M. Bandurraga and Y. S. Wu, Yucca Mountain Site Characterization Project Report, LBNL-40376, UC-814, Lawrence Berkeley National Laboratory, Berkeley, CA.

Wu, Y. S., Chen, G., Haukwa, C. and Bodvarsson, G. S., 1996a. Three-dimensional model calibration and sensitivity studies, Chapter 8 of "Development and calibration of the three-dimensional site-scale unsaturated-zone model of Yucca Mountain, Nevada" Edited by G. S. Bodvarsson and M. Bandurraga, Yucca Mountain Site Characterization Project Report, Lawrence Berkeley National Laboratory, Berkeley, CA.

Wu, Y.S., C.F. Ahlers, P. Fraser, A. Simmons, and K. Pruess, 1996b. Software qualification of selected TOUGH2 Modules. Ernest Orlando Lawrence Berkeley National Laboratory, LBNL-39490.